AIAA JOURNAL
Vol. 49, No. 5, May 2011

Adaptation of the Beveled Nozzle for High-Speed Jet Noise Reduction

K. Viswanathan* and M. J. Czech†
The Boeing Company, Seattle, Washington 98124-2207

DOI: 10.2514/1.J050409

The noise of high-speed jets, generated by nozzle exhaust systems that resemble typical jet engine installations on fighter aircraft, has been investigated with the main objective of developing noise reduction designs. To this end, the aeroacoustic characteristics of beveled nozzles have been examined in model scale tests, and their performance relative to a conventional round nozzle system has been established. Two different physical models with appropriate area ratios to simulate the engine operating conditions at different power settings were tested; these correspond to 96% N1 (military power) and 91% N1 (cutback power). Aeroacoustic measurements and analyses have been carried out for nozzles at bevel angles of 20, 24, 28, and 35° for military power, and 24 and 32° for cutback power. For the same plenum conditions, the mass flow rates for the beveled nozzles are identical to those of the baseline round nozzle, for a wide range of nozzle pressure ratio. The thrust coefficients are higher for the beveled nozzles for both the nozzle geometries at typical military power and cutback power, respectively. The increase in the thrust coefficient ranges from ∼0.75% for the bevel35 to ∼2% for bevel28, in spite of the slight deflection of the jet plume. The reasons for this phenomenon are examined. The beveled nozzles produce at least the same or greater absolute thrust as the baseline nozzle. The beveled nozzles specifically reduce the noise in the peak polar radiation angles; the maximum noise benefit is observed in the azimuthal direction of the longer lip. The magnitude of noise reduction increases with increasing bevel angle, with the largest reduction for bevel35. An examination of the dBA metric, which is used in noise exposure studies, indicates that there is a noise benefit of ∼3 to ∼4 dBA in the peak radiation sector. The noise benefit in the azimuthal direction of the shorter lip is only slightly lower than that in the direction of the longer lip, while there is a small noise increase toward the broader side of the beveled nozzle at the lower inlet angles.

I. Introduction

THE noise of high-speed jets, as from the engines that power fighter aircraft, is a major concern for both military personnel and civilians living close to military bases. Military jets are powered by turbojets or very low bypass-ratio turbofan engines (BPR ≤ 0.3). The attendant high jet velocities produce extremely high levels of jet noise. This problem is severe for operations on aircraft carrier decks because military personnel are stationed very close to the aircraft during the launch and the landing of carrier-based fighter aircraft. Pilots perform training missions, called Field Carrier Landing Practice, at military bases that mimic the actual flights at the appropriate engine power settings, thereby creating a huge noise problem for the surrounding communities. The magnitude of the problem is first highlighted with a comparison of the noise footprints from the F/A-18 A/B and the Boeing 737–800 aircraft. The noise foot print is calculated as follows: first, A-weighted spectra are calculated from the measured spectra over a wide range of radiation angles. The A-weighting adjusts the full-scale spectrum measured by the microphone to account for the response of the human ear, with the low frequency levels decreased by several decibels, and the high-frequency portion of the spectrum relatively unmodified. The energy levels in the resulting spectrum at the different frequencies are logarithmically summed to produce one dBA number at each angle. The maximum dBA levels are calculated at several points on a grid on the ground and contours of noise levels in dBA are produced using the Integrated Noise Model. Figure 1 shows the contours for a single landing and takeoff, with the areas inside the contours representing exposure to noted levels or higher. The inset table lists the contour areas in square miles. Typically, the 65-dBA contour defines the maximum allowable noise level and the challenge is to shrink this boundary as much as possible. The huge difference in the noise levels due to the difference in the bypass ratio between a turbojet and a high BPR turbofan engine is immediately evident from this figure. Whereas the area of the 65-dBA contour is 34 square miles for the B737-800, it is 193 square miles for the F/A-18. Each division represents 10,000 ft (∼2 miles) as noted; with an average width of ∼4 miles, the 65-dBA contour extends to ∼50 miles under the flight path. Therefore, there is a pressing need to reduce the noise impact of these aircraft and provide relief to the affected communities.

The nozzles of jet engines that power fighter aircraft are invariably operated at off-design conditions at low altitudes, thereby generating shock-associated noise in addition to turbulent mixing noise. There are three principal noise components for an imperfectly expanded supersonic jet. These are the turbulent mixing noise, the broadband shock-associated noise, and the screech tones. The intensity of the shock-associated noise is dependent on the degree of mismatch between the design Mach number M_d and the fully expanded jet Mach number M_j. The relative importance of the broadband shock-associated noise and turbulent mixing noise is a strong function of the radiation angle and the jet operating conditions. The shock noise radiation peaks at lower inlet angles, while the mixing noise is radiated principally to the aft directions. However, the mixing noise level is considerably higher even for shock-containing jets. Figure 2 shows the directivity of the overall sound pressure level (OASPL) for typical nozzle geometry at typical takeoff power, referred to as military (MIL) power here. The aircraft is assumed to fly on a straight level flight at an altitude of 1000 ft. All polar angles are measured from the jet inlet axis. Two curves, one at static conditions and the other at a flyover Mach number of 0.233 are shown. For the static case, the peak level at ∼130° is ∼15 dB higher than those at the lower radiation angles. Note that the turbulent mixing noise is the dominant component in the peak radiation sector in the aft quadrant. For the case with forward flight, the difference in level is still roughly 12 dB.

Presented as Paper 2010-654 at the 48th AIAA Aerospace Sciences Meeting, Orlando, FL, 4–7 January 2010; received 31 December 2009; revision received 18 September 2010; accepted for publication 12 December 2010.

*Boeing Technical Fellow; M/S 0R-JF, P.O. Box 3707; k.viswanathan@boeing.com. Associate Fellow AIAA.

†Aeroacoustics Engineer; M/S 0R-JF, P.O. Box 3707; michael.j.czech@boeing.com. Member AIAA.

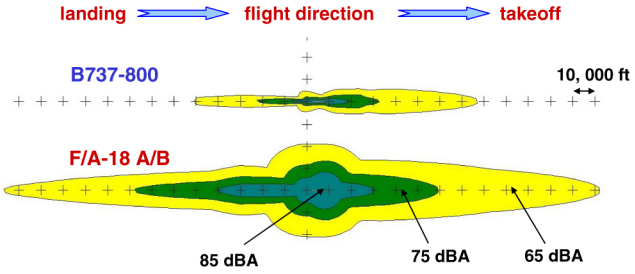

	B737-800	F/A-18 A/B
85 dBA	1.7	19.4
75 dBA	7.0	61.0
65 dBA	34	193

Fig. 1 Comparison of noise footprints from the Boeing B737-800 and the F/A-18 A/B from a single flyover event. The direction of flight is from left to right. The inset table lists the contour areas in square miles.

The reduction in the mixing noise level due to forward flight is seen to be ∼4 dB at the peak angles. Figure 3 shows a comparable plot for the directivity of the dBA, again at MIL power. The trends are very similar: the mixing noise component in the peak radiation direction is ∼10 dB higher than the levels in the low angles. The main message from these two figures is the following: the mixing noise in the peak radiation sector must be reduced to mitigate the noise impact of fighter aircraft.

Recently, Viswanathan [1–3] proposed the beveled nozzle for jet noise reduction and carried out detailed aeroacoustic tests; both single-stream and dual-stream nozzles were considered. To gain better insights into the modifications to the flow and radiated noise, large eddy simulations for the same nozzle geometries have been carried out; see [4] for complete details. The salient results for a single jet from a convergent beveled nozzle are first reviewed. Noise measurements, over a wide range of polar angles, were made at several azimuthal angles to map the azimuthal variations. The performances of the beveled nozzles were assessed against a reference round nozzle. The beveled nozzles introduce significant azimuthal variations in the spectra, resulting in major differences in the polar directivities of the overall sound pressure levels at different azimuthal angles; these differences become pronounced when the jet velocity is increased. Significant noise reduction (both in the overall power

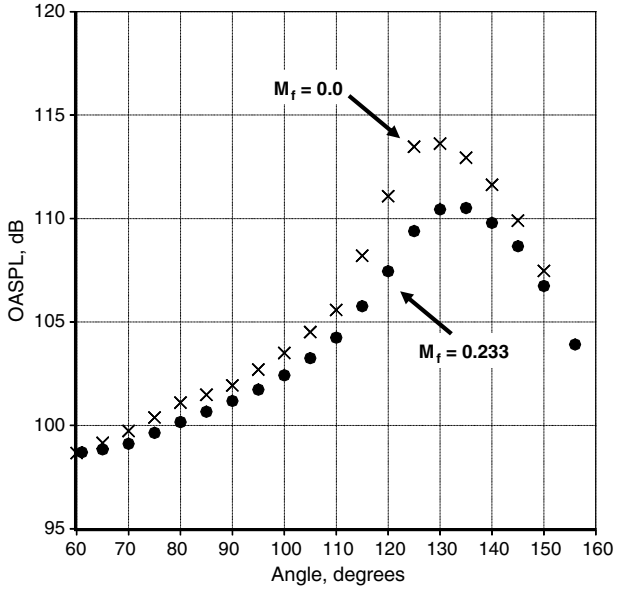

Fig. 2 Directivity of the overall sound pressure level at MIL power. Flight Mach numbers of 0.0 and 0.233.

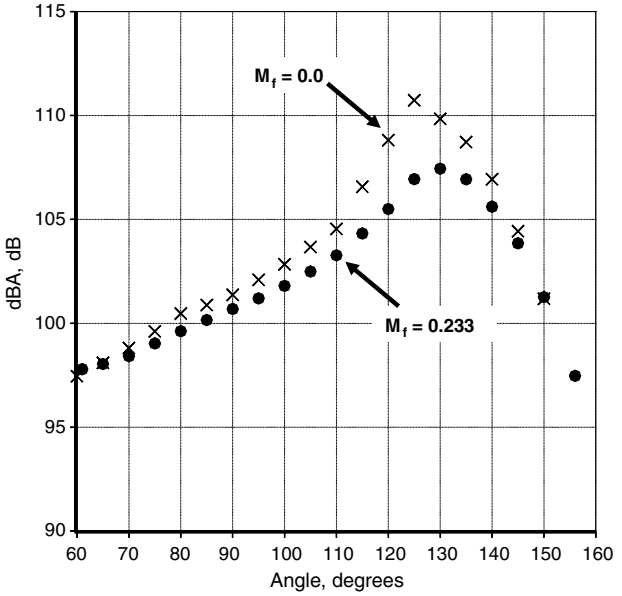

Fig. 3 Directivity of the dBA at MIL power. Flight Mach numbers of 0.0 and 0.233.

level, and the directivity of the perceived noise level) is achieved in the azimuthal directions below the longer lip of the beveled nozzle, principally in the polar angular range of ∼110–∼140°. Furthermore, this reduction is observed at all frequencies. The magnitude of the noise reduction is a strong function of the jet velocity, with progressively higher reductions as the jet velocity is increased. With proper orientation of the nozzle, the noise footprint on the ground can be reduced.

As noted in section IV.D of Viswanathan [1], asymmetric nozzles have been considered for the elimination of screech tones and the possible alleviation of broadband shock-associated noise. Norum [5] tested a variety of tube nozzles with different modifications to the geometry of the trailing edge and demonstrated large reductions in screech amplitude. Wlezien and Kibens [6] investigated the flow and noise characteristics of two beveled nozzles ("inclined" nozzles in their terminology) and several tabbed nozzles and noted substantial azimuthal variation. At a polar angle of 90°, the asymmetry of the screech tone was found to be responsible for the azimuthal variation of OASPL. Rice and Raman [7,8] attempted to reduce noise from supersonic unheated jets by promoting enhanced mixing through the use of beveled nozzles and the introduction of paddles into the shear layer (thus producing intense screech tones) of rectangular jets. The intended application was for an ejector. With the beveled nozzle, even though there was a reduction in noise at the lower frequencies, there was a substantial increase (∼10 dB) of broadband high-frequency noise at the lower angles. The main goal of the above studies of asymmetric nozzles was the attainment of enhanced mixing, with potential application for thrust vectoring for fighter aircraft and possible noise reduction. It is important to note that even though enhanced mixing was attained and screech tones either eliminated or reduced in amplitude, all these studies failed to yield broadband noise reduction, as demonstrated by Viswanathan [1–3]. Furthermore, all these studies were restricted to unheated jets.

Simple convergent nozzles were considered in the preceding investigation of [1–3]. In this study, the beveled nozzle is adapted to the exhaust geometry that is typical of the engines with high specific thrust that power fighter aircraft. Detailed aeroacoustic measurements and analyses have been carried out for nozzles with several bevel angles. There is substantial reduction of noise in the peak radiation sector; secondly, there is an improvement in the uninstalled static thrust performance for all the bevel angles considered. It should be kept in mind, however, that the external drag differences should be taken into account when assessing system-level performance. The effects of installation have not been evaluated, as these were beyond the scope of this study.

II. Experimental Program

The experiments are performed in the Low-Speed Aeroacoustic Facility at Boeing, with simultaneous measurement of thrust and noise. Descriptions of the test facility, the jet simulator, the data acquisition and reduction process, etc., may be found in Viswanathan [9–11]. The jet simulator is embedded in an open-jet wind tunnel, which can provide a maximum freestream Mach number of 0.32. Bruel & Kjaer Type 4939 microphones are used for free-field measurements. The microphones are set at normal incidence and without the protective grid; this setup yields a flat frequency response up to 100 kHz. Since we anticipate significant azimuthal variation, two microphone arrays 30° apart in the azimuthal direction are employed. The microphones in one array are laid out at a constant sideline distance of 15 ft (4.572 m) from the jet axis; the microphones in the other are on a polar arc at a distance of 25 ft (7.62 m). All angles, measured from the jet inlet axis, cover a polar angular range of 50–150°. The exit diameter of the nozzle is 4.0° (10.16 cm), with a corresponding microphone distance of 75D for the polar array. Note that given the large distance to the microphones, the discrepancy in polar angle between the top and bottom of the beveled nozzle is negligible. Narrowband data with a bandwidth of 23.4 Hz are acquired and synthesized to produce 1/3-octave spectra, with a center band frequency range of 200–80, 000 Hz. For comparisons at model scale, the data are corrected to a common distance of 20 feet (6.096 m) from the center of the nozzle exit (coordinate system with origin at the center of the nozzle exit) and standard-day conditions: ambient temperature of 77°F (298°K) and relative humidity of 70%. The atmospheric attenuation coefficients are obtained from the method of Shields and Bass [12]. The data are also extrapolated to full-scale conditions of the jet engine considered. The measurements from the baseline and modified nozzles are carried out at the appropriate engine cycle conditions and at realistic forward-flight velocity.

Figure 4 shows a drawing of the baseline convergent-divergent (CD) nozzle geometry; this nozzle represents a simplified version of the exhaust system of the F-414 turbojet engine that powers the fighter aircraft. Shown in the schematic sketch of the exhaust geometry, are the flow path, the centerbody and the convergent-divergent sections. This model is mated with the jet rig, with appropriate adapters and spool pieces. In the actual engine installed on the aircraft, the nozzle throat area may be varied; the nozzle exit area also varies and the ratio of these two areas is a function of the engine thrust setting (represented by fan rotational speed N1). In model scale testing, with fixed throat and exit areas, it therefore becomes necessary to build different physical models with appropriate area ratios to simulate the engine operating conditions at different power settings. Two different baseline nozzle geometries that correspond to 96% N1 (MIL power) and 91% N1 (cutback power) were tested. The ratio of the exit area to the throat area at 96% N1 is 1.398; the corresponding theoretical design Mach number for this area ratio is 1.76 (NPR = 5.41). Four different bevel nozzles with bevel angles of 20, 24, 28. and 35° have been tested with this nozzle system (denoted as nozzle system one), with and without a flight stream. The ratio of the exit area to the throat area at 91% N1 is 1.224; the corresponding theoretical design Mach number for this area ratio is 1.56 (NPR = 4.0). Two beveled nozzles with bevel angles of 24 and 32° were tested with this nozzle system (denoted as nozzle system two). The exit area for the beveled nozzle is taken to be the geometric area in the slant plane. The definitions of the various angles (polar, azimuthal and bevel) are illustrated in Fig. 5.

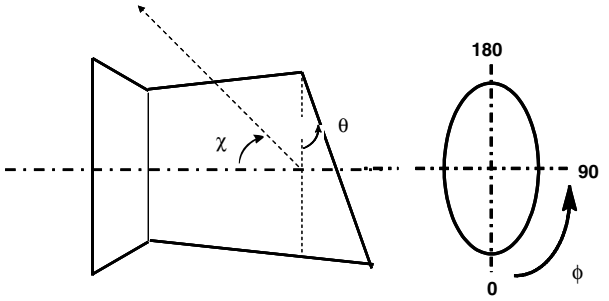

Fig. 5 Conceptual sketch of a beveled nozzle and the measurement convention for the polar angle χ, bevel angle θ, and the azimuthal angle ϕ.

III. Results and Discussion

In the past, most concepts for jet noise reduction have invariably incurred unacceptable performance penalty. The biggest challenge is to minimize the thrust degradation of any concept; in addition, the suitability for retrofit opportunities must be considered. One of the principal goals of this study is the development of nozzle concepts that do not incur a performance penalty or at most have a minor negative impact. Therefore, special care was taken in the thrust measurements, as described below. The thrust performance is first presented; then the acoustic results are described.

A. Aerodynamic Performance

First, the force balance was calibrated by applying a known force and measuring the response of the balance. The applied force was incremented by 100 lbf, starting from 0 to 1400 lbf. Then the applied load was decreased 100 lbf stepwise, so as to document hysteresis effects, if any. This exercise was carried out twice, the first time before the start of the test and the second time after the completion of the test. Figure 6 shows the calibration curve; there are two sets of circles (pretest calibration) and two sets of triangles (posttest calibration). The straight line is the ideal response, with a 45° slope. As seen, there is excellent linear response and the average error for the calibration is ±0.13%. In general, the maximum error in the thrust measurements can be taken to be less than ±0.20%, though it can be actually lower. Additional information may be found in section III.B of [9].

The measured thrust is used to calculate the thrust coefficient as follows. For a nozzle operating at a nozzle pressure ratio of (p_t/p_a) and reservoir temperature ratio of (T_t/T_a), the throat Mach number M is given by

$$M = \sqrt{\frac{2}{(\gamma-1)}\left[\left\{\frac{p_t}{p_a}\right\}^{\left(\frac{\gamma-1}{\gamma}\right)} - 1\right]} \quad \text{for} \quad \left\{\frac{p_t}{p_a}\right\} < \left(1+\frac{\gamma-1}{2}\right)^{\frac{\gamma}{\gamma-1}} \tag{1}$$

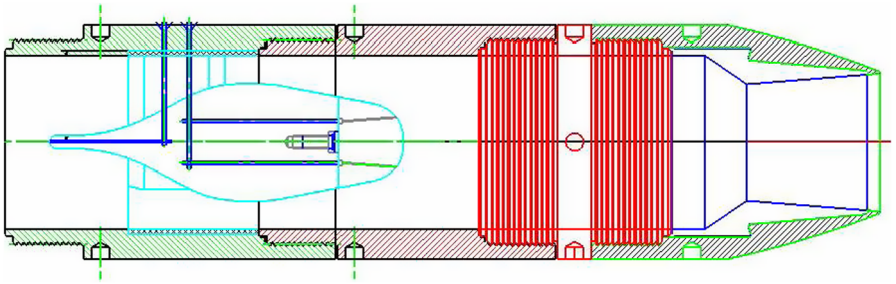

Fig. 4 Schematic sketch of the exhaust system, with the flow path and the centerbody.

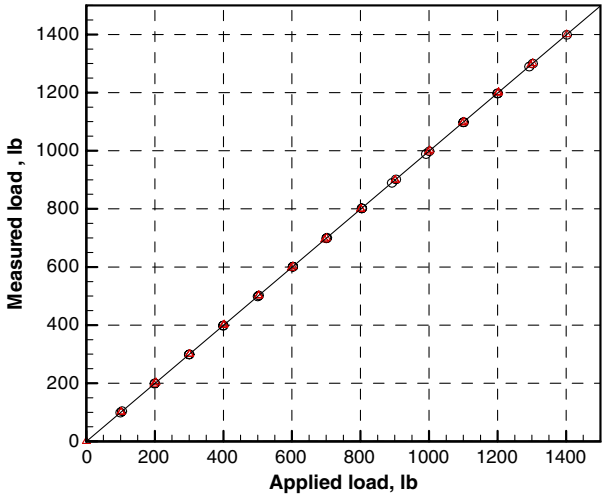

Fig. 6 Calibration of force balance showing measured load versus applied load. o: pretest; Δ: posttest.

$$M = 1, \quad \text{for } \left\{\frac{p_t}{p_a}\right\} \geq \left(1 + \frac{\gamma - 1}{2}\right)^{\frac{\gamma}{\gamma - 1}} \tag{2}$$

From the gas dynamic equations, the expressions for the ideal mass flow rate $\dot{m}$, ideal jet velocity V_j, and ideal thrust F may easily be derived in terms of the nozzle reservoir conditions. These quantities may be expressed as follows:

$$\dot{m} = p_t A M \sqrt{\frac{\gamma}{RT_t}\left[1 + \frac{\gamma - 1}{2} M^2\right]^{-\left(\frac{\gamma+1}{2(\gamma-1)}\right)}} \tag{3}$$

$$V_j = \sqrt{2RT_t\left(\frac{\gamma}{\gamma - 1}\right)\left[1 - \left\{\frac{p_t}{p_a}\right\}^{-\left(\frac{\gamma-1}{\gamma}\right)}\right]} \tag{4}$$

$$F = \dot{m} V_j \tag{5}$$

$$F = p_t A M \gamma \left[1 + \frac{\gamma - 1}{2} M^2\right]^{-\left(\frac{\gamma+1}{2(\gamma-1)}\right)} \sqrt{\left(\frac{2}{\gamma - 1}\right)\left[1 - \left\{\frac{p_t}{p_a}\right\}^{-\left(\frac{\gamma-1}{\gamma}\right)}\right]} \tag{6}$$

In the above expressions, p_t is the plenum total pressure, A is the throat area, T_t is the plenum total or stagnation temperature, R is the gas constant, and γ is the ratio of specific heats. The thrust coefficient is defined as

$$C_f = \frac{F_{\text{measured}}}{\dot{m}_{\text{measured}} * V_j} \tag{7}$$

First, we need to verify that the beveled nozzles would generate the same axial thrust as the baseline round nozzle. For given plenum conditions (NPR and total temperature ratio T_t/T_a), the measured mass flow rates should be the same for the baseline and the beveled nozzles. Figure 7 shows the measured mass flow rates and the corrected mass flow rates for the five different nozzles. The corrected mass flow rates W_c are calculated as per the usual definition, at standard day conditions of T_{std} and p_{std} as:

$$W_c = \frac{W_{\text{actual}} * \sqrt{T_t/T_{\text{std}}}}{p_t/p_{\text{std}}} \tag{8}$$

In Fig. 7, the measured mass flow rates increase with NPR as expected; there is a slight variation for the different nozzles due to small variations in the ambient conditions and small differences in the nozzle operating conditions. However, there is a tight collapse for

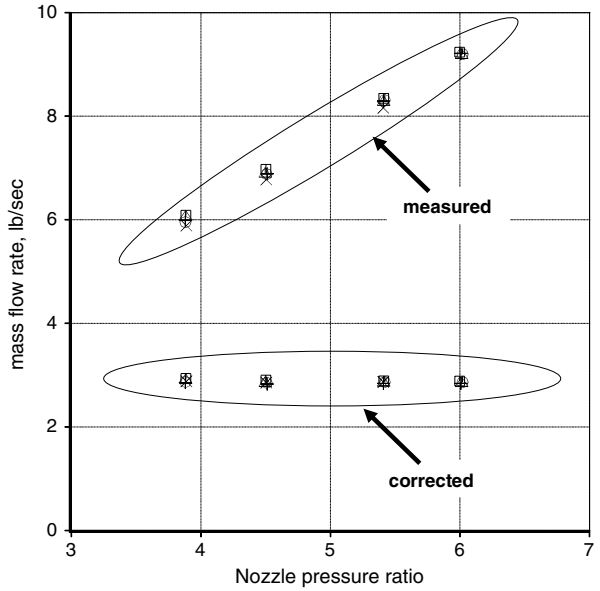

Fig. 7 Measured and corrected mass flow rates at different NPR. o: round; x: bevel20; □: bevel24; Δ: bevel28; +: bevel35. Nozzle system one, 96% N1.

the corrected mass flow rates. Perhaps this is not unexpected because the convergent-divergent nozzles are operated at choked pressure ratios and the mass flows are controlled by the throat area.

Figure 8 shows the repeatability of the thrust measurements from the four beveled nozzles (nozzle system one) over a range of NPR. There is tight collapse of the nozzle thrust coefficients for the bevel20 (circles) and bevel35 (triangles) nozzles; there is slightly larger scatter for the other two nozzles. However, the scatter is still of the same order as the accuracy of the balance measurements. Figure 9 shows a comparison of the thrust performance of the baseline and beveled nozzles again over a range of NPR. The nozzle pressure ratios that correspond to the MIL power and the ideally expanded jet are also identified in this figure. The performance of the baseline nozzle, denoted by the letter A and a curve-fit, follows the typical trend for a CD nozzle: the thrust coefficient peaks close to the ideally expanded NPR and drops off as the jet becomes progressively over and underexpanded. Note that the polynomial fit seems to show a peak at a slightly higher NPR; this is an artifact of the curve-fit, and

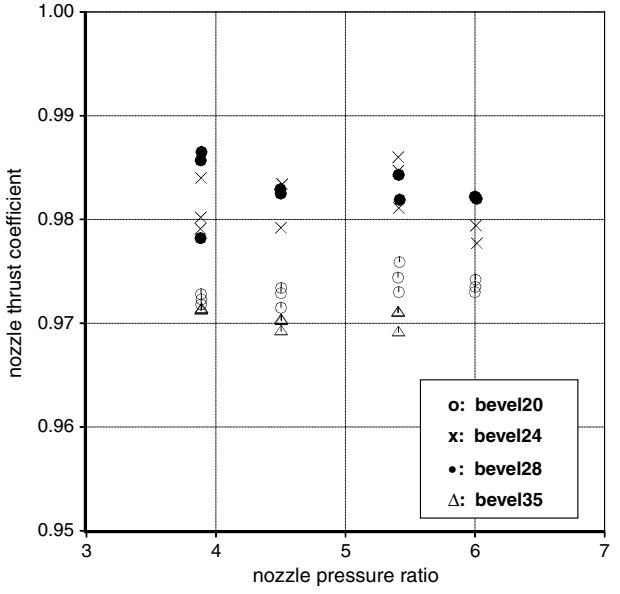

Fig. 8 Repeatability of thrust measurements from beveled nozzles. Nozzle system one, 96% N1.

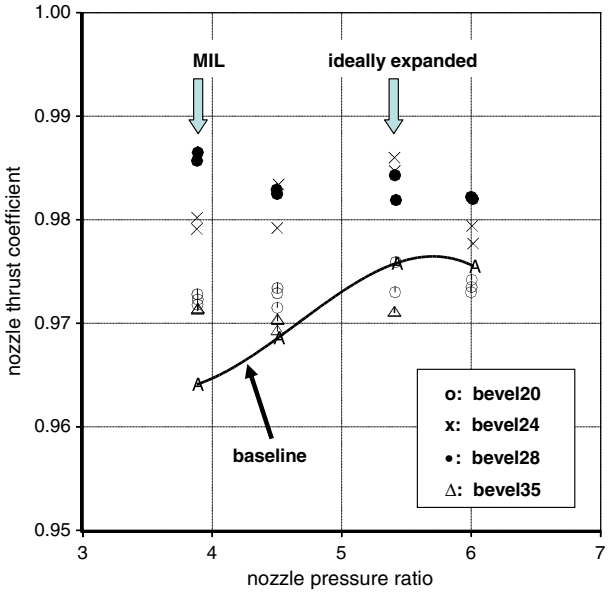

Fig. 9 Comparison of the thrust coefficients of the beveled and baseline nozzles. Nozzle system one, 96% N1.

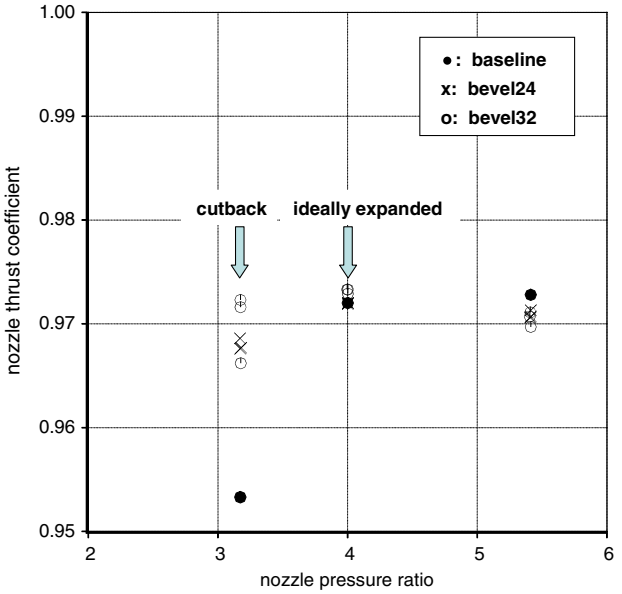

Fig. 11 Comparison of the thrust coefficients of the beveled and baseline nozzles. Nozzle system two, 91% N1.

measurements at closely spaced NPR would be necessary to identify the exact design Mach number of the nozzle. It is also evident that all the beveled nozzles have a higher thrust coefficient at MIL power, when compared with the round nozzle. The increase in the thrust coefficient ranges from ∼0.75% for the bevel35 to ∼2% for bevel28. Further, there is an increase in the thrust coefficient at the higher NPRs for most of the test points shown. This increase in performance is relative to the given baseline nozzle geometry; similar levels of improvements may not be always possible.

Comparable results from the second nozzle system, with an area ratio of 1.224, are now presented. Figure 10 shows the measured and corrected mass flow rates at three nozzle pressure ratios. The trends are very similar to those shown in Fig. 7 for the nozzle system one: there is excellent agreement of the mass flow rates for the round and beveled nozzles. Figure 11 presents a comparison of the nozzle thrust coefficients from the beveled and the baseline nozzles. The nozzle pressure ratios that correspond to the cutback power and the ideally expanded jet are highlighted in this figure. There is enhanced thrust performance for the two beveled nozzles: ∼1.5% for bevel24 and ∼1.9% for bevel32.

Through a combined examination of Figs. 7–11 and Eqs. (3–8), the following conclusions may be reached. The ideal thrust is given by the product of the measured mass flow rate and the ideal jet velocity. The ideal jet velocity depends only on the plenum conditions [see Eq. (4)]; the measured mass flow rates are the same for the round and beveled nozzles (see Figs. 7 and 10]. Therefore, the ideal thrust on the denominator of Eq. (7) is invariant for fixed plenum conditions. The variation of the thrust coefficient with NPR is shown in Figs. 9 and 11: the thrust coefficients of the beveled nozzles are better than those of the round nozzle at overexpanded conditions. The trends indicate that the measured absolute thrust produced by the beveled nozzle [numerator of Eq. (7)] is higher than or at least equal to that generated by the round nozzle. Therefore, the measurements from the two nozzle systems indicate that 1) the beveled nozzles produce at least the same absolute thrust as the baseline round nozzle, and 2) the beveled nozzles exhibit better thrust performance relative to the round nozzle.

The reason for the observed increase in nozzle thrust coefficient is now examined. Attention is drawn to the fact that the pressure distribution at the (slanted) exit plane of the beveled nozzle is nonuniform, with a pressure gradient in the vertical direction for the nozzle orientation as shown in Fig. 5. Recall that convergent beveled

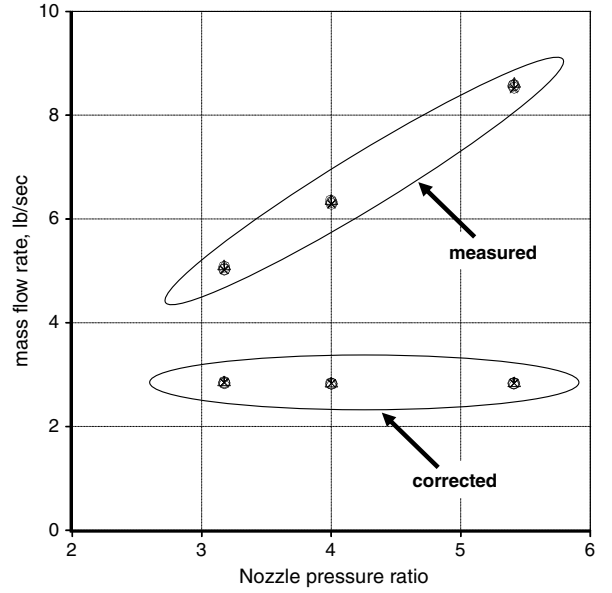

Fig. 10 Measured and corrected mass flow rates at different NPR. Δ: round; x: bevel24; o: bevel32. Nozzle system two, 91% N1.

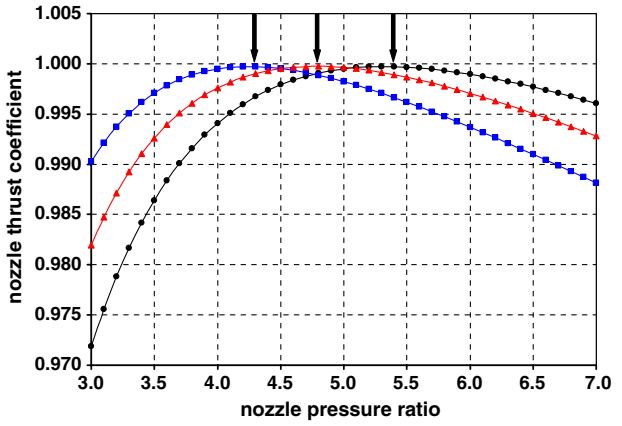

Fig. 12 Variation of the ideal thrust coefficient with NPR for nozzles with different ratios of exit to throat areas. •: $A_e/A_t = 1.398$; ▲: $A_e/A_t = 1.328$; ■: $A_e/A_t = 1.258$.

nozzles were tested in [1]. It is possible to measure the actual mass flow rate for given plenum conditions with a critical flow venturi. The measured mass flows provide a good estimate of the "effective" flow area, which is more pertinent than the geometric exit area, as can be appreciated from an examination of Eq. (3). From precisely such a measurement in Viswanathan [1] for the round and beveled nozzles, it was determined that the effective flow area is lower than the geometric flow area for the beveled nozzle. Figure 5 indicates that the flow would actually reach the nozzle exit sooner at the top than at the bottom, thus establishing a more complex flow field. This phenomenon could explain the drop in the flow rates for the beveled nozzles, with the more severe bevel angle producing a greater reduction. See section III in [1] for more details. The main observation is the following: the effective flow area for the beveled nozzle is lower than the geometric area because of the nonuniform pressure distribution at the nozzle exit plane. The magnitude of the reduction in the flow area and the resulting reduction in corrected mass flow rate were confirmed by Navier–Stokes computations in [4]. The situation is different for the convergent-divergent nozzles used in the present investigation. As already shown in Figs. 7 and 10, the mass flow rates are not affected by the beveled trailing edge when the CD nozzles are operated at supercritical NPR, with the nozzles choked. However, the effective exit flow area is reduced and it is lower than the geometric area (in the slanted plane that coincides with the beveled trailing edge). This reduction in exit flow area has a beneficial effect for thrust performance for the following reason. The nozzles of the typical engines are operated at overexpanded NPR at sea-level and low-altitude flight regimes; only at cruise conditions is the NPR close to being perfectly expanded. With a reduction in the effective exit area due to beveling, the nozzles are operated closer to the ideally expanded area ratio, thereby reducing the shock strength and improving the aerodynamic performance. Figure 12 shows the performance of an ideal nozzle as a function of NPR, with a given area ratio of 1.398 (denoted by black circles). As expected, the peak thrust coefficient is obtained for the ideally expanded NPR of 5.4. Note that the ideal thrust coefficient, based on one-dimensional analysis, is close to unity; of course, this is not the case in real life. Two other performance curves, with reductions in area ratios of 5% (triangles) and 10% (squares) are also shown in Fig. 12. The nozzle pressure ratios that correspond to the ideally expanded conditions, highlighted by black arrows, are lower for these cases. The thrust performance is better for these nozzles, with lower area ratios, over a wide range of NPR that corresponds to overexpanded conditions for the original nozzle with area ratio of 1.398. The experimental measurements are in accord with the trends observed in Fig. 12.

Table 1 Variation of the plume deflection angle with NPR for different nozzles

	Bevel20	Bevel24	Bevel28	Bevel35
NPR	θ, deg	θ, deg	θ, deg	θ, deg
3.89	−1.65	−1.72	−1.47	−0.85
4.50	−0.76	−0.60	−0.25	−0.51
5.41	0.23	0.65	1.17	2.56
6.00	0.69	1.20	1.79	——
Total angle	1.88	2.37	2.64	3.41

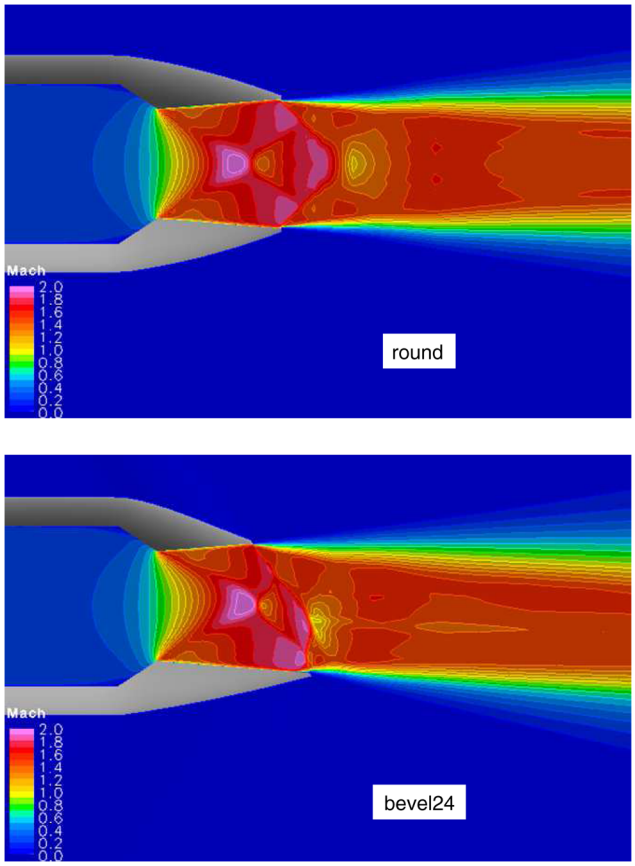

Fig. 13 Comparison of computed Mach number contours at MIL power. Top: baseline nozzle; bottom: bevel24 nozzle.

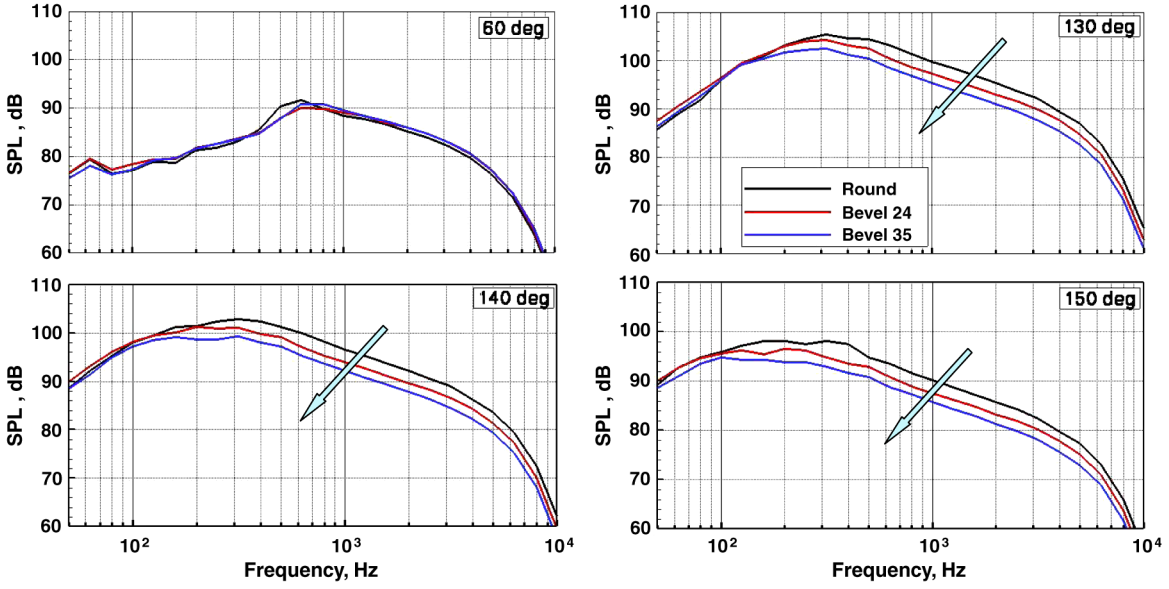

Fig. 14 Comparison of spectra at MIL power from nozzle system one. $M_f = 0.0$.

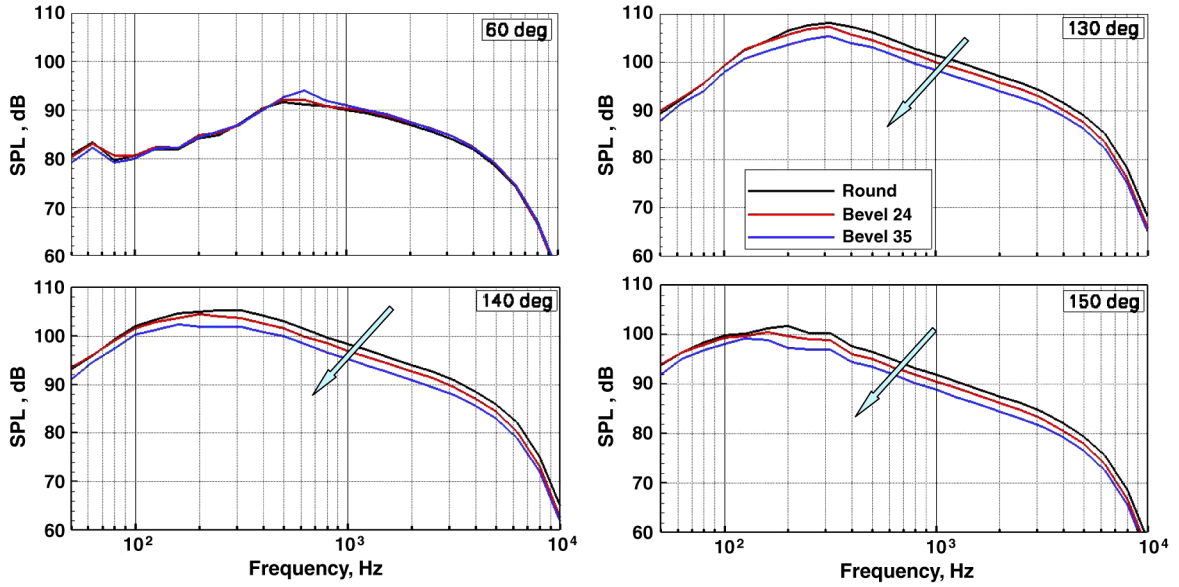

Fig. 15 Comparison of spectra at design Mach number (NPR = 5.41) from nozzle system one. $M_f = 0.0$.

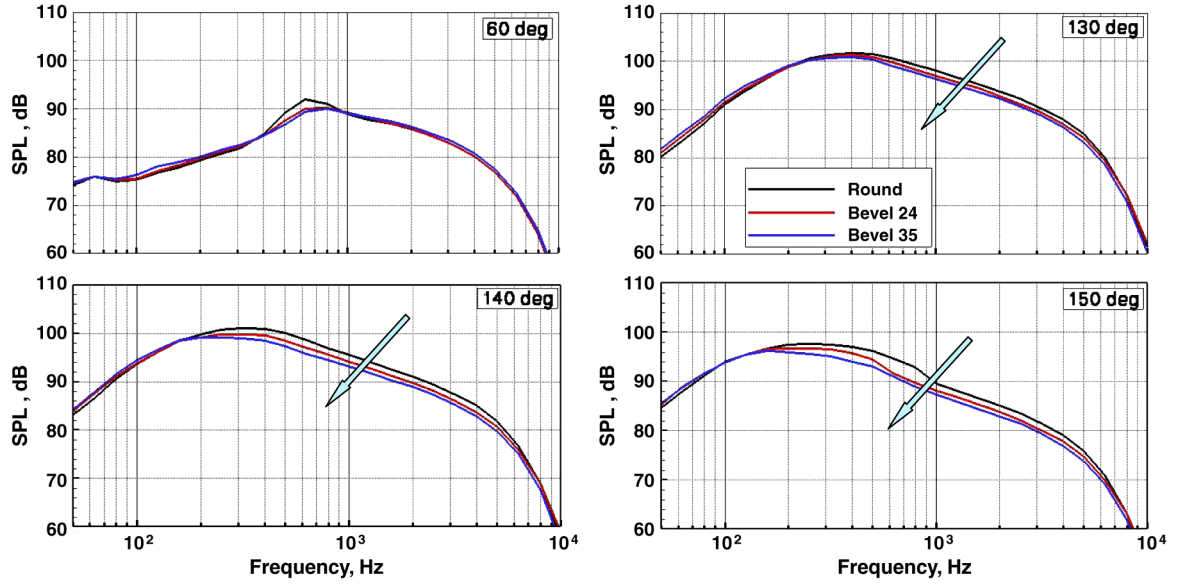

Fig. 16 Comparison of spectra at MIL power from nozzle system one. $M_f = 0.233$. Round, bevel20, and bevel28 nozzles.

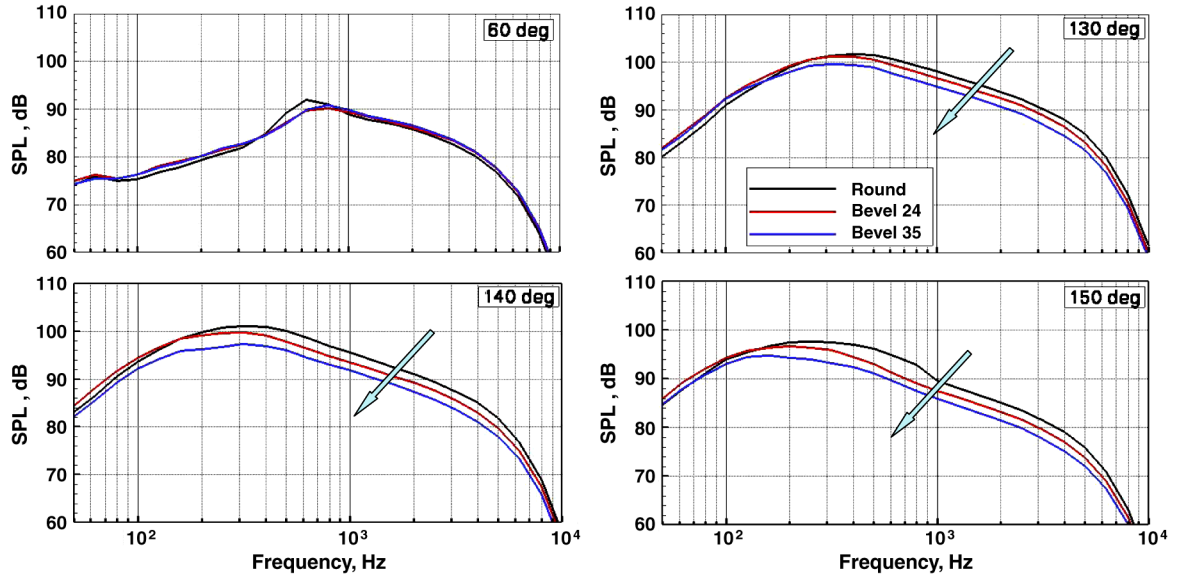

Fig. 17 Comparison of spectra at MIL power from nozzle system one. $Mf = 0.233$. Round, bevel24, and bevel35 nozzles.

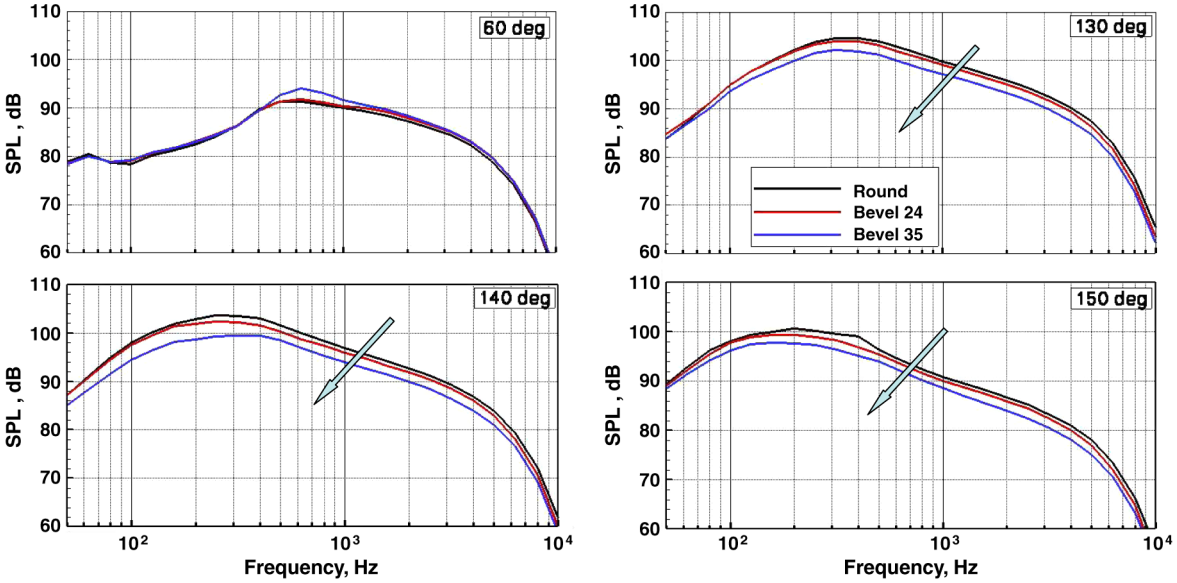

Fig. 18 Comparison of spectra at design Mach number (NPR = 5.41) from nozzle system one. $M_f = 0.233$. Round, bevel24, and bevel35 nozzles.

It is also worth noting that the ideal performance curves are fairly flat near the correctly expanded NPR. That is, the difference in thrust performance would be small when the nozzle is operated in the vicinity of the correctly expanded NPR. In the jet engines that power fighter aircraft, both the convergent and divergent portions consist of straight-walled sections; see Fig. 4. For such geometry, shocks are always present, even at the theoretical fully expanded NPR. This observation is borne out when the spectra at the lower polar angles in the forward quadrant are examined in section III.B. The above flow features and the aerodynamic performance of straight-walled CD nozzles provide insights to the trends observed in Figs. 9 and 11.

The second issue pertains to the plume deflection due to the beveling. Viswanathan [1] showed that the jet plume is deflected toward the shorter side of the beveled nozzle for convergent nozzles. Further, the angle of plume deflection is more pronounced for larger bevel angles. Several video cameras were installed in the anechoic chamber, though no flow surveys were carried out. The pictures indicated that the plume is deflected toward the longer side of the beveled nozzle at MIL power. The thrust axes for these nozzles do not coincide with the geometric centerline of the round nozzle: additional forces are produced in the normal directions in the cross-sectional plane, which have been measured with the six-component force balance. The measured forces are used to estimate the angle of plume deflection.

In addition, Navier–Stokes simulations for the baseline and beveled nozzles have been carried out. The Boeing Computational Fluid Dynamics flow analysis software package is used for the computational fluid dynamics analyses. Viscous effects are modeled using the shear stress transport two-equation turbulence model. The Liu–Vinokur equilibrium air chemistry model is used to take into account variations of air chemistry with temperature. The effects of combustion products are ignored, as these effects are thought to be negligible for the conditions analyzed. A sample comparison of the computed flowfields, in terms of Mach number distributions for the baseline and bevel24 nozzles at MIL power, is shown in Fig. 13.

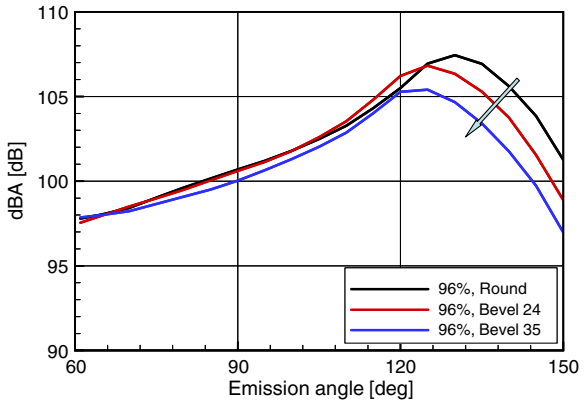

Fig. 19 Variation of dBA with emission angle for the round, bevel24, and bevel35 nozzles. MIL power, $M_f = 0.233$.

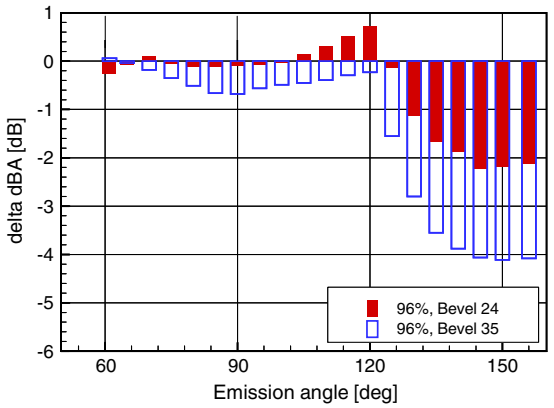

Fig. 20 Noise benefit due to the beveled nozzles, dBA metric. Bevel24 and bevel35 nozzles. MIL power, $M_f = 0.233$. Azimuthal angle = 0°.

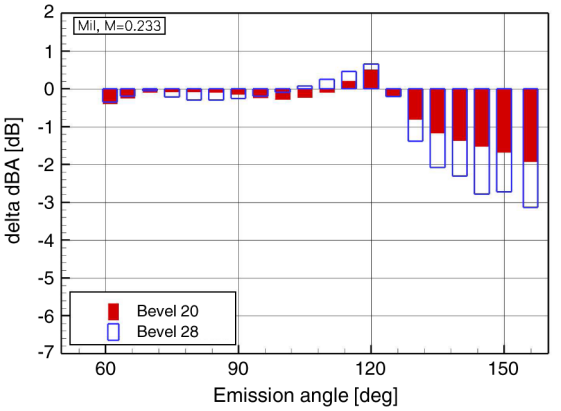

Fig. 21 Noise benefit due to the beveled nozzles, dBA metric. Bevel20 and bevel28 nozzles. MIL power, $M_f = 0.233$. Azimuthal angle = 0°.

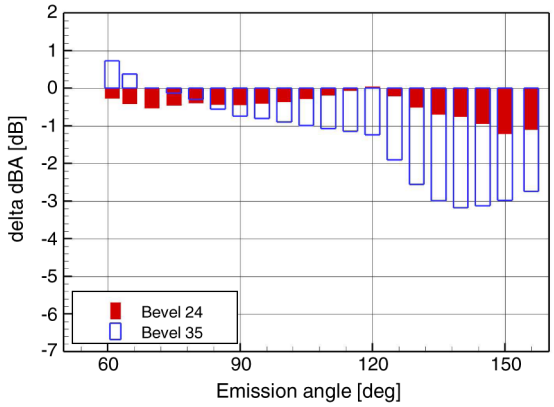

Fig. 22 Noise benefit due to the beveled nozzles, dBA metric, NPR = 4.5. Bevel24 and bevel35 nozzles. $M_f = 0.233$. Azimuthal angle = 0°.

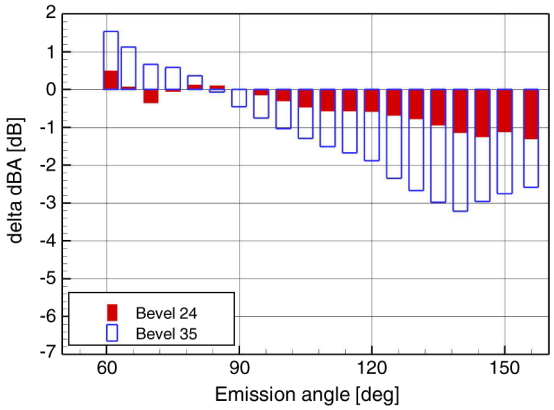

Fig. 23 Noise benefit due to the beveled nozzles, dBA metric at design Mach number (NPR = 5.41). Bevel24 and bevel35 nozzles. $M_f = 0.233$. Azimuthal angle = 0°.

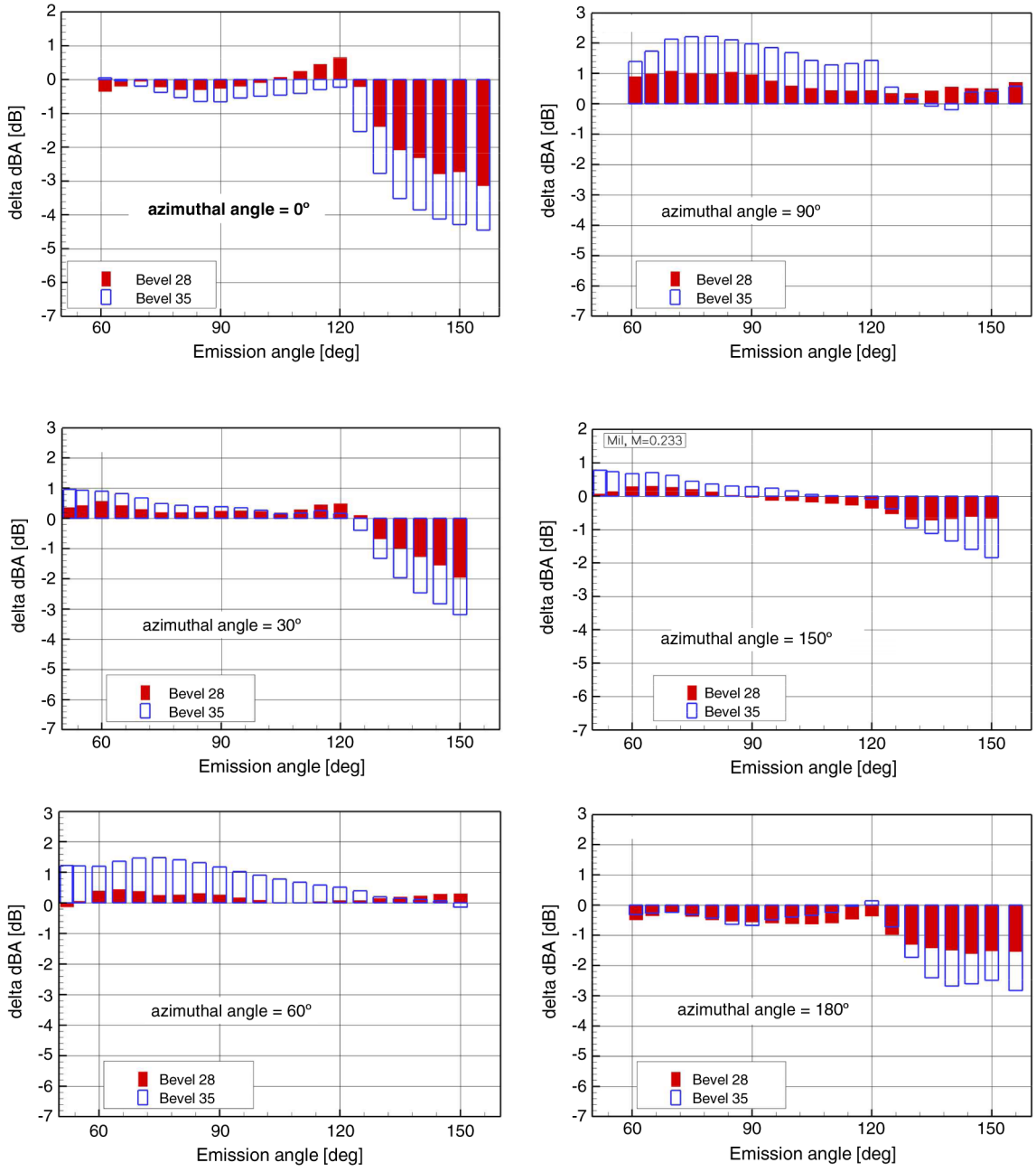

Fig. 24 Noise benefit due to the beveled nozzles, dBA metric. Bevel28 and bevel35 nozzles. MIL power, $M_f = 0.233$. Various azimuthal angles.

For the overexpanded jet, the plume contracts immediately downstream of the nozzle exit plane for the round nozzle; the formation of a Mach disc is also evident. For the beveled nozzle, the plume again contracts at the short lip as the jet exits the nozzle. However, the plume is still inside the nozzle in the longer lip direction (vertical plane) and the Mach disc is displaced downward. The resulting slight deflection of the plume toward the long lip due to the beveling of the nozzle is evident. There is an important difference in the direction of plume deflection: whereas the plume deflects toward the short lip direction for convergent nozzles, the plume deflects in the opposite direction for the CD nozzle for overexpanded conditions. As the NPR is progressively increased, the deflection angle becomes smaller with respect to the horizontal axis and eventually the plume deflects toward the short lip for underexpanded jets.

The following deflection angles have been determined for the beveled nozzles, for the four nozzle pressure ratios shown in Fig. 9. The deflection angle is taken to be negative if the plume deflects downward toward the longer lip, for the nozzle orientation shown in Fig. 5. First, a brief discussion of the operation of the engines that power the F/A-18 is pertinent. The nozzles are operated at overexpanded NPR during takeoff and low-altitude flights. At "cruise" conditions, the NPR is close to the ideally expanded value. Table 1 provides a summary of the measured deflection angles; an underexpanded NPR is included for the sake of information, but the total deflection angle covers only the overexpanded to ideally expanded regime.

Note that the plume deflection angles are very small, of the order of $\pm 1.5°$ in general. That is, the normal forces are small. The flow situation is very different for the CD beveled nozzles, with the plume deflection angle being small even for large bevel angles. In contrast, the plume deflection angle keeps increasing with bevel angle for convergent beveled nozzles. Attention is drawn to the fact that the axial thrust coefficient is slightly smaller, and equal to the cosine of the deflection angle. Given the small angles, though, this loss of thrust is negligible [cosine of (1.5°) is 0.9997]. There are two effects on aerodynamic performance due to beveling: 1) decrease in the effective exit flow area, and 2) a small deflection of the plume.

Let us reexamine Fig. 9: the thrust coefficients of the beveled nozzles are higher than that of the round nozzle at both the overexpanded conditions, and comparable to those of the round nozzle at the ideally expanded and underexpanded NPR. Similar trends are observed for the second nozzle system in Fig. 11. These results indicate that the counteracting effect of area modification more than overcomes the effect of plume deflection, thereby assuring good thrust performance over a wide range of NPR. It is important to keep in mind that the nozzles on the jet engine are operated at overexpanded NPR in most flight regimes; at cruise the NPR is close to ideally expanded conditions.

B. Acoustics

A variety of noise metrics are presented for the various nozzle geometries and for several cycle conditions. These consist of the spectra, the directivities of OASPL and dBA, the noise benefit in terms of dBA, and finally the reductions in the effective perceived noise level (EPNL). The measured spectra, with the 20% scale-model of the engine, have been extrapolated to full-scale conditions. The aircraft is assumed to fly on a level trajectory at a fixed altitude of 1000 ft. Because data have been acquired up to 80 kHz, the maximum full-scale frequency is 16 kHz. Note that the integrated noise metrics cover the frequency range of 50 Hz–10 kHz. First, spectral comparisons are presented at static conditions; four polar angles of 60, 130, 140, and 150° cover a wide range. Figures 14 and 15, respectively, show full-scale spectra at MIL power and at the design M_d for nozzle system one. Unless otherwise noted, the azimuthal angle is 0°, in the direction of the long lip of the beveled nozzle. The arrows indicate the direction of increasing bevel angle in these and following figures. There are minor modifications to the spectra at 60° due to beveling; similar trends are observed at all the angles in the forward quadrant. As we move aft, there is a reduction in levels at all the frequencies. The magnitude of the noise reduction is more pronounced in the peak radiation sector; hence the choice of the polar angles. Similar spectral trends are observed at both power settings.

Figures 16 and 17 show spectral comparisons in the presence of a flight stream; the flight Mach number M_f is 0.233. The acoustic performance is assessed for all the beveled nozzles; bevel20 and bevel28 in Fig. 16 and bevel24 and bevel35 in Fig. 17, respectively. The following trends are observed in these two figures: 1) there are only slight modifications to the spectra at 60° (and at lower polar angles, not shown), similar to the trend seen for static conditions; 2) the magnitude of the noise reduction increases with increasing bevel angle, with the largest reduction for bevel35; 3) the beveled nozzles reduce noise at all frequencies, without any increase at the higher frequencies; and 4) the spectral trends in the aft quadrant (noise reduction) are also similar to those observed under static conditions. Figure 18 shows a comparable plot at a higher NPR (=5.41), at the design Mach number. Again, the trends are very similar to those seen in Fig. 17 for an overexpanded jet.

The variation of the dBA metric, which is used in noise exposure studies, is now presented. Figure 19 shows a comparison of the

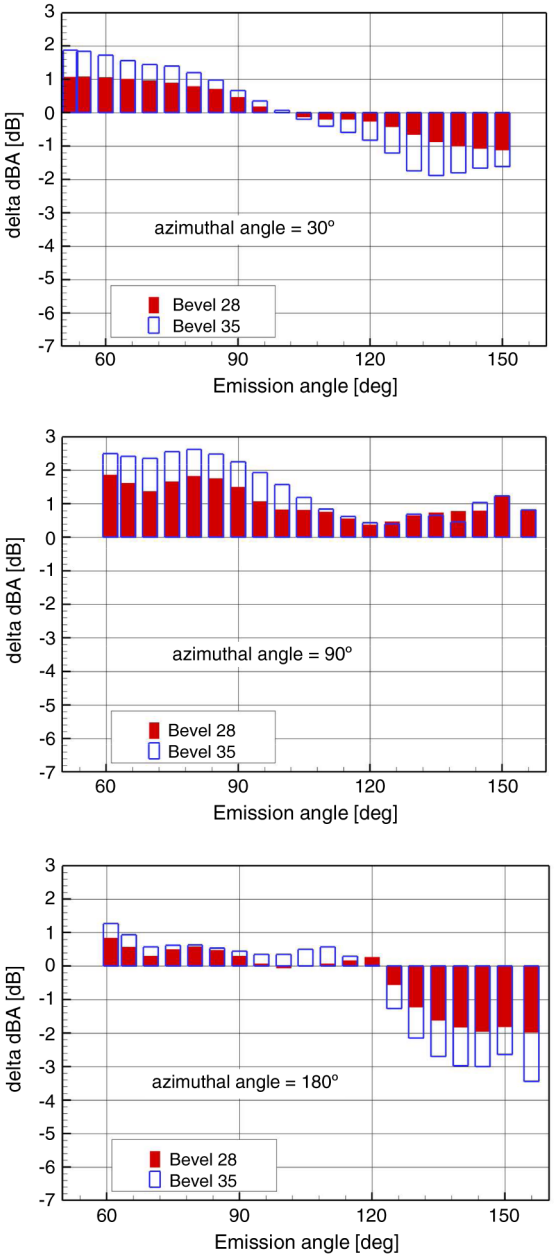

Fig. 25 Noise benefit due to the beveled nozzles, dBA metric at design Mach number (NPR = 5.41). Bevel28 and bevel35 nozzles. $M_f = 0.233$. Various azimuthal angles.

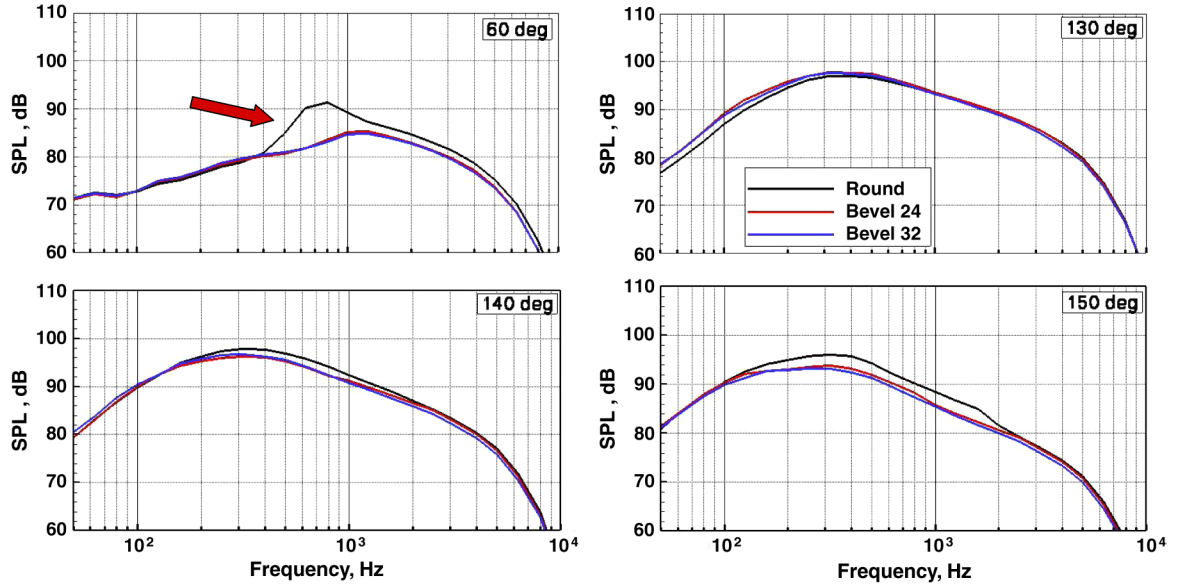

Fig. 26 Comparison of spectra at 91% N1 (NPR = 3.171) power from nozzle system two. $M_f = 0.233$. Round, bevel24 and bevel32 nozzles.

directivity of the dBA metric for the round, bevel24, and bevel35 configurations; the flight Mach number is 0.233. Consistent with the spectral trends, there is only a minor change at the lower angles; however a reduction of ∼4 dBA is observed in the peak radiation sector. The change in noise levels, relative to the round nozzle, at all the radiation angles is shown in Fig. 20. As seen, the noise reduction is confined to the peak radiation sector for this nozzle. For the sake of completeness, a similar plot for the other two beveled nozzles at MIL power is shown in Fig. 21. The trends are similar for all the beveled nozzles: 1) there are only minor modifications at the lower polar angles; 2) the reduction in noise is confined to the peak radiation sector; and 3) there is a monotonic increase in the magnitude of the noise benefit with increasing bevel angle. Comparable plots at two higher NPRs of 4.5 and 5.41 (design Mach number) are shown in Figs. 22 and 23, respectively. At these higher NPR, there is a slight reduction in the noise benefit: the magnitude is ∼3 dB for bevel35 at these higher NPR.

From the acoustic data presented so far, we see that the two beveled nozzles with bevel angles of 28 and 35 deg provide larger magnitudes of noise benefit. The azimuthal variations of the noise change in the dBA metric are examined for these two nozzles now. Figures 24 and 25 show such variations at azimuthal angles of 0, 30, 60, 90, 150, and 180° for the MIL power, and at a reduced number of angles for NPR = 5.41, respectively. The following trends may be discerned: 1) there is a reduction of noise benefit as we move to increasingly larger azimuthal angles, from 0 to 90°; 2) at 90°, there is a noise increase of ∼2 dBA in the forward quadrant and ∼1 dBA at the aft angles; 3) there is a noise reduction at 150°; 4) at 180°, there is noise benefit of ∼3 dBA in the peak radiation sector, with only a slight change in levels at the lower radiation angles. The results indicate that the beveled nozzle yields a noise benefit in the directions of both the long and short lips in the azimuthal plane.

These trends suggest the following possible orientations for the beveled nozzle for a fighter aircraft with twin-podded engines, such as on the F/A-18. Both the beveled nozzles can be installed with the longer lip toward the ground: 1) then, the noise benefit will be the greatest in the peak radiation sector, ∼4 dBA for the bevel35 (see Fig. 20); 2) the slight plume deflection must be accounted for in some fashion. Alternately, one nozzle would have the longer lip toward the ground and the other one with the shorter lip toward the ground: 1) the noise benefit in the peak radiation sector will be slightly reduced (see Figs. 20 and 24); 2) however, the effects of the small plume deflections will exactly cancel each other out, because they are in the opposite directions. An added concern then is the introduction

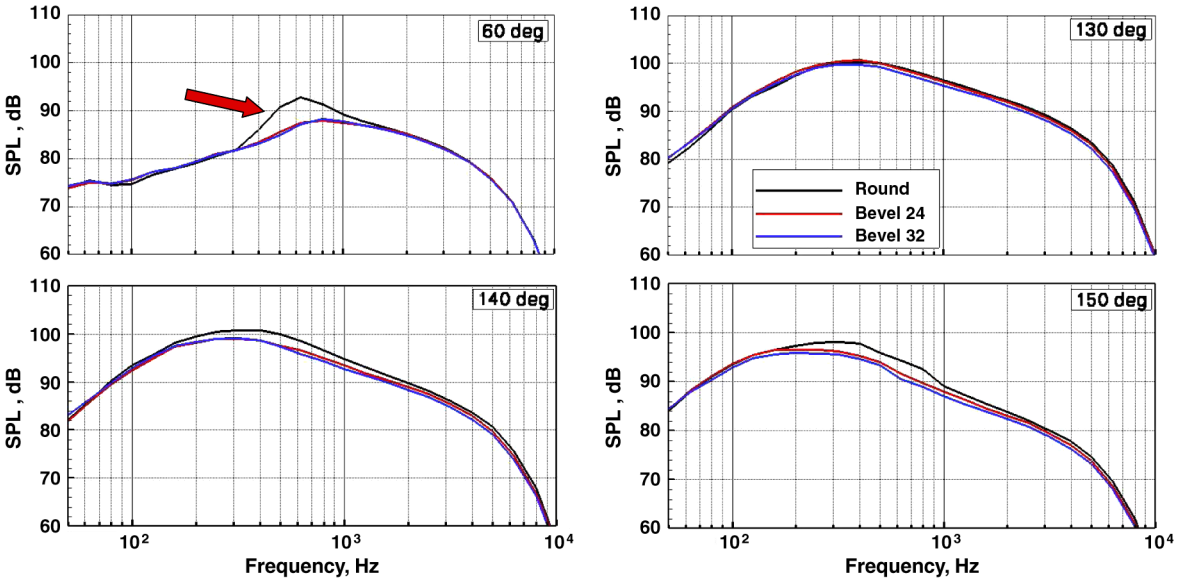

Fig. 27 Comparison of spectra at NPR = 4.0 (design Mach number) from nozzle system two. $M_f = 0.233$. Round, bevel24, and bevel32 nozzles.

of a rolling moment, because of the lateral offset between the two nozzle centerlines. If a reduction of the noise exposure for the crew on an aircraft carrier deck is desired, a different orientation of the beveled nozzles would be preferred. Because the nozzles are at about the same height above the carrier deck as the crew members, the beveled nozzles would be oriented with the longer lips parallel to the ground and facing outward: azimuthal angles of 90° for the right engine and 270° for the left engine (when looking forward from behind the engines), respectively. With this arrangement, the opposing sideward forces will exactly cancel each other. A detailed investigation of twin-podded jets is essential first; a system-level study of all the integration issues must then be carried out.

A few sample results obtained with the nozzle system two, with ratio of the exit area to the throat area of 1.224, are now presented. As with nozzle system one, spectral comparisons are first shown in Figs. 26 and 27 at two nozzle pressure ratios of 3.171 (91%N1) and 4.0 (design Mach number), respectively. There is a clear reduction in the shock peak at 60°, at both NPR. This trend is contrary to that seen for nozzle system one. As noted in the section on aerodynamic performance, there is a reduction in the effective exit flow area resulting in 1) substantially improved thrust performance for severely overexpanded jets; and 2) a better flow expansion with reduced shock strengths for overexpanded jets. One would expect a reduction in shock-associated noise for off-design operation from this consideration. However, this effect is manifested only for nozzle system two. The following discussion offers a possible explanation. The shock strength is usually characterized by the parameter $\sqrt{|M_j^2 - M_D^2|}$, raised to some exponent. The value of the exponent has been believed to be 4; recent measurements and analyses by Viswanathan et al. [13] indicated, however, that the exponent has a dependence on both the polar angle and the jet temperature ratio. Regardless, the value of the shock parameter is 0.69 at cutback power and 0.85 at MIL power. It appears that the reduction in shock-associated noise could be associated with the shock strength, with the beveled nozzles being effective for jets with weaker shocks.

The noise benefit in the dBA metric for the above two NPR are depicted in Figs. 28 and 29, respectively. At the NPR of 3.171, there is significant benefit at the lower polar angles due to the reduction of shock-associated noise; the magnitude of this reduction reaches ∼4 dB at 60°. At the peak radiation sector, the level of reduction is between ∼2 and ∼3 dB. At the theoretical design Mach number (NPR = 4.0), shocks are still present for the baseline nozzle; the beveled nozzles yield ∼2 dB noise benefit in the forward quadrant. In the aft quadrant, the magnitude of the benefit is comparable to that seen for NPR = 3.171.

Finally, the effect of the beveled nozzles on the EPNL (EPNdB) metric is shown. Even though this metric is used for the certification of commercial aircraft, the results are included for the sake of completeness and because many researchers are familiar with this noise metric. Figure 30 shows the benefit, relative to the baseline round nozzle, for all the beveled nozzles at MIL power and for

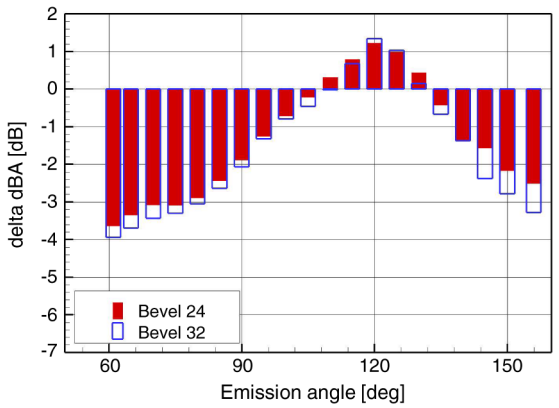

Fig. 28 Noise benefit due to the beveled nozzles, dBA metric, NPR = 3.171. Nozzle system two; bevel24 and bevel32 nozzles. $M_f = 0.233$.

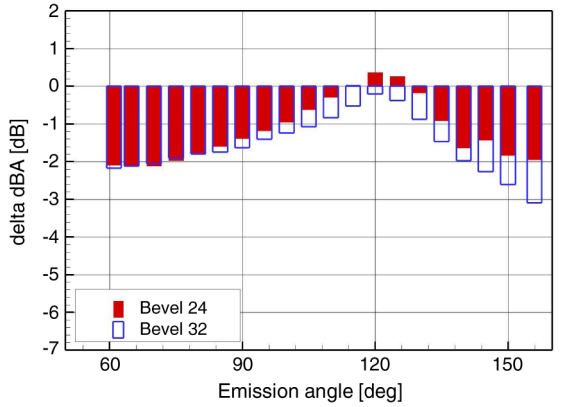

Fig. 29 Noise benefit due to the beveled nozzles, dBA metric, NPR = 4.0. Nozzle system two; bevel24 and bevel32 nozzles. $M_f = 0.233$.

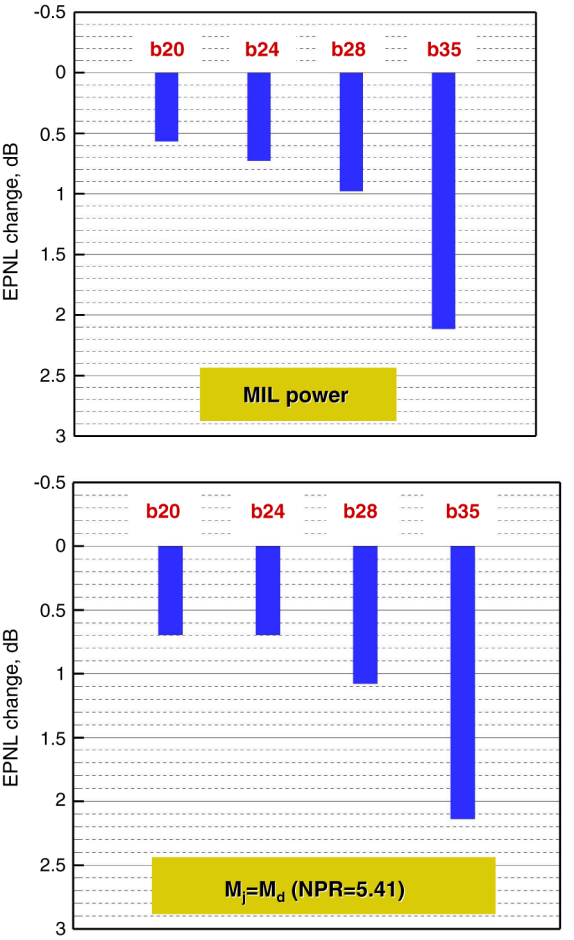

Fig. 30 Benefit in the EPNL metric. $M_f = 0.233$. Top: MIL power; bottom: NPR = 5.41.

NPR = 5.41; the bars correspond to increasing bevel angle as we move from left to right. The maximum benefit is seen for bevel35, with the bevel28 nozzle the second best. The trends are consistent with those seen in the spectral plots for the various bevel nozzles.

IV. Conclusions

The noise of high-speed jets, generated by nozzle exhaust systems that resemble typical jet engine installations on fighter aircraft, has been investigated with the main objective of developing noise reduction designs. To this end, the aeroacoustic characteristics of

beveled nozzles have been examined and their performance relative to a conventional round nozzle system has been established. Two different physical models with appropriate area ratios to simulate the engine operating conditions at different power settings have been considered; these two correspond to 96% N1 (MIL power) and 91% N1 (cutback power). Detailed aeroacoustic measurements and analyses have been carried out for nozzles with several bevel angles: bevel angles of 20, 24, 28, and 35° at MIL power, and 24 and 32° at cutback power. Furthermore, both nozzles have been operated over a wide range of nozzle pressure ratios to gain insights to their performance.

For the same plenum conditions, the mass flow rates for the beveled nozzles are identical to that of the baseline round nozzle, for a wide range of NPR. There are two effects on the plume due to beveling: 1) a slight deflection of the plume, and 2) a small reduction in the effective nozzle exit area. Both measurements and computations indicate that the plume deflects toward the longer lip of the convergent–divergent beveled nozzles operated at supercritical pressure ratios. This deflection is in the opposite direction to that observed for convergent beveled nozzles. The deflection angle is small, even for large bevel angles, and is of the order of $\pm 1.5°$. For overexpanded jets at MIL power, the deflection angle has the maximum value. As the NPR is progressively increased, the plume angle decreases and finally the plume deflects toward the short lip of the beveled nozzle. The measurements indicate that the thrust coefficients are substantially higher for the beveled nozzles for both the nozzle geometries at typical MIL power and cutback power, respectively. The increase in thrust coefficient ranges from $\sim 0.75\%$ for the bevel35 to $\sim 2\%$ for bevel28. Further, there is an increase in thrust coefficient at the higher NPRs for most of the test points. The small loss in axial thrust due to the plume deflection is more than compensated by the enhanced thrust performance due to the reduction in effective flow area for the beveled nozzles. In summary, it is noted that the deflection angle is small, the thrust coefficient is much better, and the beveled nozzles produce at least the same absolute thrust as the baseline nozzle.

The typical nozzles that power fighter aircraft are operated at overexpanded NPRs at MIL power and during low-altitude operations. Shocks are present, consequently generating shock-associated noise. However, the turbulent mixing noise which is dominant in the peak radiation sector is ~ 10–~ 15 dB higher than the noise radiated to lower polar angles where shock-associated noise is dominant. The beveled nozzles specifically reduce the noise in the peak radiation angles. Several noise metrics such as the spectra, A-weighted noise levels, and the EPNLs have been examined, at both static and typical flight Mach numbers. The maximum noise benefit is observed in the azimuthal direction of the longer lip. The following effects of the beveling on noise spectra are observed: 1) there are only slight modifications to the spectra at the lower polar angles; 2) in the peak polar radiation sector, the magnitude of the noise reduction increases with increasing bevel angle, with the largest reduction for bevel35; 3) the beveled nozzles reduce noise at all frequencies, without any increase at the higher frequencies; and 4) the spectral trends are similar for static and forward-flight conditions. An examination of the dBA metric, which is used in noise exposure studies, indicates that there is a noise benefit of ~ 3–~ 4 dBA in the peak radiation sector. There is also a commensurate benefit in the EPNL metric. For the nozzle system one (MIL power), there are only minor changes to the spectra in the forward quadrant. However, for the nozzle system two (cutback power), there is significant noise benefit at the lower angles as well. The reason for this benefit is attributed to the lower shock strength at this test condition.

The azimuthal variations in the radiated noise have also been examined. The following results are established: 1) there is an erosion of noise benefit as we move to increasingly larger azimuthal angles, from 0 (longer lip direction) to 90°; 2) at 90°, there is a noise increase of ~ 2 dBA in the forward quadrant and ~ 1 dBA at the aft angles; and 3) at 180°, again there is a noise benefit of ~ 3 dBA in the peak radiation sector, with only a slight change in levels at the lower radiation angles.

In closing, it is established here that there is substantial reduction of noise in the peak radiation sector; secondly, there is an improvement in the static thrust performance for all the bevel angles considered. Detailed studies of twin-podded jets must be undertaken, and possible implementation options for a typical aircraft must be assessed at the system level.

Acknowledgments

This project has been funded by the U.S. Office of Naval Research; Gabriel Roy is the Technical Monitor. The Boeing Company served as a subcontractor to the Florida State University, the prime Contractor; Anjaneyulu Krothapalli is the Principal Investigator at Florida State University. The computational simulations were carried out by Mark Reissig and David Mayer of The Boeing Company.

References

[1] Viswanathan, K., "Nozzle Shaping for Reduction of Jet Noise from Single Jets," *AIAA Journal*, Vol. 43, No. 5, 2005, pp. 1008–1022. doi:10.2514/1.11331

[2] Viswanathan, K., "An Elegant Concept for Reduction of Jet Noise from Turbofan Engines," *Journal of Aircraft*, Vol. 43, No. 3, May–June 2006, pp. 616–626. doi:10.2514/1.11432

[3] Viswanathan, K., "Noise of Dual-Stream Beveled Nozzles at Supercritical Pressure Ratios," *Journal of Aircraft*, Vol. 43, No. 3, May–June 2006, pp. 627–638. doi:10.2514/1.11433

[4] Viswanathan, K., Shur, M., Spalart, P. R., and Strelets, M., "Flow and Noise Predictions for Single and Dual-Stream Beveled Nozzles," *AIAA Journal*, Vol. 46, No. 3, 2008, pp. 601–626. doi:10.2514/1.27299

[5] Norum, T. D., "Screech Suppression in Supersonic Jets," *AIAA Journal*, Vol. 21, No. 2, 1983, pp. 235–240. doi:10.2514/3.8059

[6] Wlezien, R. W., and Kibens, V., "Influence of Nozzle Asymmetry on Supersonic Jets," *AIAA Journal*, Vol. 26, No. 1, 1988, pp. 27–33. doi:10.2514/3.9846

[7] Rice, E. J., and Raman, G., "Mixing Noise Reduction for Rectangular Supersonic Jets by Nozzle Shaping and Induced Screech Mixing," AIAA Paper 93-4322, 1993.

[8] Rice, E. J., and Raman, G., "Supersonic Jets from Beveled Rectangular Nozzles," ASME Paper No. 93-WA/NCA-26, 1993.

[9] Viswanathan, K., "Jet Aeroacoustic Testing: Issues and Implications," *AIAA Journal*, Vol. 41, No. 9, 2003, pp. 1674–1689. doi:10.2514/2.7313

[10] Viswanathan, K., "Aeroacoustics of Hot Jets," *Journal of Fluid Mechanics*, Vol. 516, No. , Oct. 2004, pp. 39–82. doi:10.1017/S0022112004000151

[11] Viswanathan, K., "Instrumentation Considerations for Accurate Jet Noise Measurements," *AIAA Journal*, Vol. 44, No. 6, 2006, pp. 1137–1149. doi:10.2514/1.13518

[12] Shields, F. D., and Bass, H. E., "Atmospheric Absorption of High Frequency Noise and Application to Fractional-Octave Band," NASA-CR 2760, 1977.

[13] Viswanathan, K., Alkislar, M. B., and Czech., "Characteristics of the Shock Noise Component of Jet Noise," *AIAA Journal*, Vol. 48, No. 1, 2010, pp. 25–46. doi:10.2514/1.38521

E. Gutmark
Associate Editor